ISSN 1029-9599, Physical Mesomechanics, 2017, Vol. 20, No. 4, pp. 447–456. © Pleiades Publishing, Ltd., 2017.
Original Text © H. Carreon, D. San Martin, F.G. Caballero, V.E. Panin, 2017, published in Fizicheskaya Mezomekhanika, 2017, Vol. 20, No. 4, pp. 11–19.

The Effect of Thermal Aging on the Strength and the Thermoelectric Power of the Ti–6Al–4V Alloy

H. Carreon[1]*, D. San Martin[2], F. G. Caballero[2], and V. E. Panin[3]

[1] *Instituto de Investigaciones Metalúrgicas (UMSNH-IIM), Ciudad Universitaria, Morelia, 58000 México*
[2] *Materalia Research Group, Department of Physical Metallurgy, Centro Nacional de Investigaciones Metalúrgicas (CENIM-CSIC), Madrid, E28040 Spain*
[3] *Institute of Strength Physics and Materials Science, Siberian Branch, Russian Academy of Sciences, Tomsk, 634055 Russia*
** e-mail: hcarreon@umich.mx*

Received September 28, 2016

Abstract—When the Ti–6Al–4V alloy is overaged at 500–600°C, nanometer-sized α_2 (Ti_3Al) particles can be homogeneously precipitated inside α phases, thereby leading to strength improvement. Widmanstätten and equiaxed microstructures containing fine α_2 (Ti_3Al) particles were obtained by overaging the Ti–6Al–4V alloy. Precipitation of α_2 (Ti_3Al) particles was monitored using thermoelectric power measurements for different aging conditions in the Ti–6Al–4V alloy. Overaging heat treatments were conducted at 515, 545 and 575°C for different aging times. In addition, overaging samples were examined by optical microscopy, scanning electron microscopy and hardness measurements. It was found that the thermoelectric power is very sensitive to the aging process in the two studied Ti–6Al–4V structures.

DOI: 10.1134/S1029959917040105

Keywords: Ti–6Al–4V alloy, strengthening, thermoelectric measurements, hardness, aging

1. INTRODUCTION

High strength titanium alloys for structural applications are generally formed by two-phases ($\alpha + \beta$). Ti–6Al–4V alloy is characterized for being sensitive to microstructural variations. Depending on heat treatment conditions different microstructures can be found, namely Widmanstätten, equiaxed and bimodal. Some parameters that affect the mechanical properties of these microstructures are the volume fraction of α and β phases, their morphology, the crystallographic arrangement, the prior β grain size, the α colony size, the α platelet thickness and the presence of martensite. Amongst these, the α colony size is one the most important microstructural parameters [1–4]. Extensive research has been performed to obtain the desired mechanical properties by tailoring the microstructure through the optimization of the heat treatments or thermomechanical control processes [5].

When Ti–6Al–4V alloy is over-aged at 500–600°C, nanometer-sized, fine, ordered α_2 (Ti_3Al) particles can be homogeneously precipitated inside α phase [6, 7]. These precipitates have a DO_{19} structure [8], and nucleate homogeneously keeping coherent relationship with α during aging. Aluminum in the Ti–6Al–4V alloy plays a role in increasing the α/β transformation temperature and in forming a region coexisting α and α_2 phases in the phase diagram because it works as an α stabilizing element. The size and interparticle spacing of α_2 are mainly affected by aging temperature and concentration of aluminum.

In this study, Widmanstätten and equiaxed microstructures were obtained by different heat treatments, and then α_2 (Ti_3Al) particles were homogeneously precipitated inside α phases by aging Ti–6Al–4V samples at 515, 545 and 575°C for different times. α_2 (Ti_3Al) precipitation process was monitored using thermoelectric power measurements on unaged and aged samples. Two different methods have been employed in this research, the lateral gradient and hot tip thermoelectric power methods. To investigate the age hardening effect of this heat treatments, Vickers hardness measurements have been also carried out in parallel in the same range of aging times.

2. THERMOELECTRIC POWER METHODS

The thermoelectric methods are based on the Seebeck effect that is commonly used in thermocouples to measure temperature. This technique allows monitoring the thermoelectric power in metallic conductor materials for those processes affected by the different types of defects present in the atomic lattice such as atoms in solid solution, precipitates and dislocations. Two different experimental devices were used in this research to measure the thermoelectric power: the lateral gradient method and the hot tip method. A schematic representation of the lateral gradient thermoelectric apparatus is given in Fig. 1a. The sample is placed between two blocks of a reference metal such as copper or iron that are subjected to a temperature gradient. The thermoelectric power value of the sample is a measure of the magnitude of the induced potential difference at the metal contacts in response to the temperature gradient across the sample. Figure 1b shows the thermal gradient produced inside the sample by using the lateral gradient method. Some advantages of the mentioned thermoelectric method are: the thermal gradient is homogeneous in the sample, the macroscopic thermoelectric power of the whole sample is measured, the measurement takes only a few seconds to be made and it is a very sensitive measurement (resolution of ~1 nV/°C) as long as some rules are respected such as thermal resistance of the sample and contact thermal resistance [9, 10].

Figure 2a shows the schematic representation of the hot tip thermoelectric measurement. One of the reference electrodes (copper) is heated by electrical means to a preset temperature of T_{tip} while the other electrode is left cold at room temperature T_c. The measurement is done quickly in a few seconds to assure that the hot reference electrode is not cooled down perceivably by the sample and that the rest of the sample beyond the close vicinity of the contact point is not warmed up perceivably. Then, the measured thermoelectric voltage due to Seebeck effect is given by

$$V = \int_{T_c}^{T_{tip}} [S_s(T) - S_r(T)]\,dT = \int_{T_c}^{T_{tip}} S_{sr}(T)\,dT, \qquad (1)$$

where T is the temperature; S_s and S_r denote the absolute thermoelectric powers of the sample and the reference electrode, respectively. Any variation in material properties can affect the measured thermoelectric voltage via $S_{sr} = S_s - S_r$, which is the relative thermoelectric power of the specimen to be tested with respect to the reference electrode. In most cases, the temperature dependence of thermoelectric power can be neglected over the range of operation and thermoelectric voltage can be approximated as $V \approx (T_{tip} - T_c)S_{sr}$. Ideally, regardless of how high the temperature difference between the junctions is, only thermocouples made of different materials, or more precisely, materials of different thermoelectric power, will generate a thermoelectric signal. This unique feature makes the simple thermoelectric tester one of the most sensitive material discriminators used in nondestructive inspection. Figure 2b shows the thermal gradient produced inside the sample by using the hot tip method. Some advantages of the above thermoelectric method are: the thermoelectric power measurement is localized and thus can be used to detect heterogeneities, possibilities to measure 2D thermoelectric power map of mas-

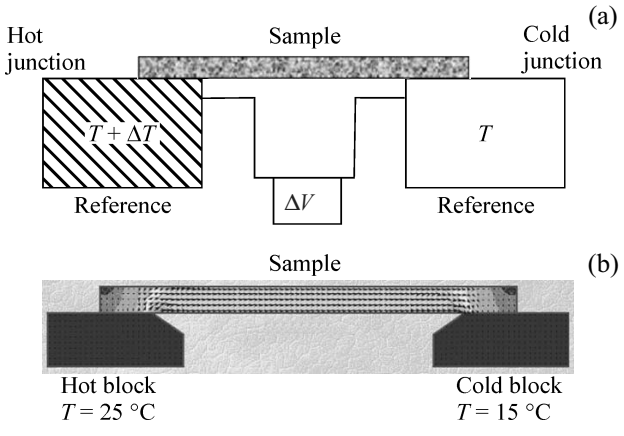

Fig. 1. Schematic diagram of the lateral gradient thermoelectric method (a) and the thermal gradient inside the sample (b).

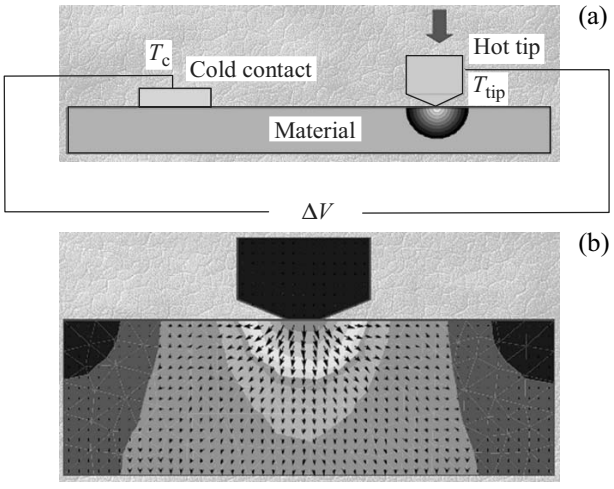

Fig. 2. Schematic diagram of the hot tip thermoelectric method (a) and the thermal gradient inside the sample (b).

sive materials, adjust the measured zone by changing the tip size, nondestructive testing possibilities directly on massive materials (in-situ measurements).

In both thermoelectric methods, the most important parameters affecting the thermoelectric measurements are those associated with volumetric and contact effects. The volumetric effect is closely related to the thermoelectricity phenomena by the kinetics of the diffusion of electrons throughout the material [11, 12]. The thermoelectric power coefficient, which is temperature-dependent, is a function of the electron scattering behavior, the electron concentration and the effective mass of the electrons. This effect is mainly affected by chemical composition, the degree of deformation of the microstructure, the presence of micro/nanoprecipitates, grain boundaries and texture [13–17]. In steels, it has also been observed that the type of crystal structure of the matrix affects the thermoelectric power significantly, which allows following solid–solid phase transformations [18, 19], in addition to precipitation and recrystallization/recovery processes [9, 10]. The contact effects are related to the imperfect contact between the test sample and the reference probe/block, amount of pressure applied to the probe/block, temperature of hot and cold junctions and probe/block material.

3. MATERIAL AND EXPERIMENTAL PROCEDURE

The material used in this study was a Ti–6Al–4V alloy plate with a thickness of 1.7 mm, supplied by Titanium Industries Inc. (USA), and its exact chemical composition is 6.19Al–4.05V–0.19Fe–0.12O–0.02C–0.01N–0.004H–Ti (wt %). Material was subjected to different heat treatments to get Widmanstätten and equiaxed microstructures and to precipitate fine α_2 intermetallic precipitates inside α phase. The Widmanstätten microstructure was obtained by holding the material at 1075°C for 15 min (above the β transformation temperature), then it was cooled down to 950°C and held for 2 h and, finally, it was water quenched. The equiaxed microstructure was obtained by holding at 700°C ($\alpha+\beta$ region), for 2 h followed by water cooling/quenching. These two microstructures were overaged at 515, 545 and 575°C for different aging times ranging from 1 min to 576 h to promote the formation of very fine α_2 (Ti_3Al) precipitates. For optical and scanning electron microscopy (SEM) inspection, heat treated samples were mounted in bakelite, ground and polished down to 1 μm diamond cloth. Microstructural features were unveiled using Kroll's reagent (H_2O 100 ml, HF 100 ml, HNO_3 100 ml). The size and volume fraction of the α and β phases was measured using an image analyzer. To evaluate microhardness variations amongst the samples, Vickers hardness measurements were performed by applying a load of 500 g on selected samples. At least three indents were performed on each sample and the average value was reported. Prior to the microhardness test, samples were cross-sectioned and metallographically prepared in a similar fashion as for optical microscopy observation, but using a much finer finishing approach with a colloidal silica solution (0.05 μm).

The lateral gradient thermoelectric power measurements were performed using a calibrated TECHLAB lateral gradient thermoelectric contact apparatus. The sample is pressed between two blocks of a reference metal (pure copper). One of the blocks is set at 15°C, while the other is at 25°C to obtain a temperature difference ΔT. A potential difference ΔV is generated at the reference metal contacts. The apparatus does not give the absolute thermoelectric power value of the sample, but a relative thermoelectric thermoelectric power value in comparison to the thermoelectric power value of pure copper at 20°C. The relative thermoelectric power value is given by Eq. (1). The measurements are performed very quickly (<1 min) and precisely (±0.5%), with a resolution of about ~1 nV/°C.

In addition, the absolute thermoelectric power of each Ti–6Al–4V specimen was also measured by using a calibrated ATS-6044T Alloy Thermo-Sorter, which provides relative readings with arbitrary units. Therefore it was firstly calibrated by materials of known absolute thermoelectric power such as copper and standard thermocouples like alumel and chromel.

The hot tip thermoelectric instrument sets up the temperature difference by means of a dual tipped reference probe. One tip is at room temperature and the other is heated to a specific temperature. In our case, a copper hot tip (standard probe) was used in order to measure the thermoelectric power of the Ti–6Al–4V overaged samples. The dual-tipped probe is placed on the Ti–6Al–4V specimen, an electric circuit is completed and a signal is generated. This signal is then processed to obtain a peak reading, which is displayed on the microvolts digital display. The reading is representative of the crystalline microstructure of the sample in this case due to the precipitation process in overaged titanium alloy samples. Each sample was measured three times and the distribution of the results was in the range of several nanovolts, while the thermoelec-

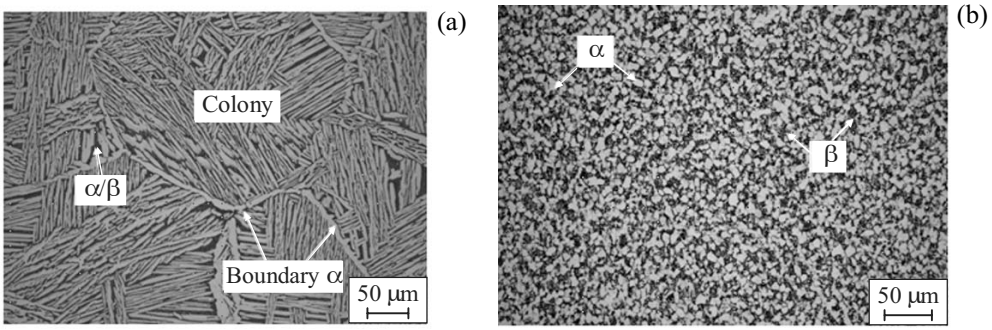

Fig. 3. Optical micrographs of the Widmanstätten (a) and equiaxed microstructures (b). Etched with Kroll's reagent. In this micrographs, α is the white/bright phase and β is the black/dark phase.

tric power values for both types of measurements were of the order of microvolts, making the measurement error negligible.

4. RESULTS

4.1. Microstructural Characterization

In Ti–6Al–4V, appreciable improvements in mechanical properties such as: strength and creep resistance can be achieved by precipitation hardening [5]. The strengthening effect critically depends on the size, volume fraction, dispersion of particles and coherency with matrix. In this respect, the promotion of α_2 phase precipitation appears to be beneficial as the optimum dispersion can be achieved by homogenization and ageing procedures.

Figure 3 shows the optical micrographs of the Widmanstätten and equiaxed microstructures. In the Widmanstätten microstructure, α phase grains (white phase) have been formed along prior β grain boundaries and colonies of lath-type β and α lamellar structure are present inside prior β grains (Fig. 3a). The colony size, the α platelets thickness and the grain boundary α phase thickness were measured to be in the range 973–1868 μm, 1–5 μm and 1–7 μm respectively. In the equiaxed microstructure, about 48% of β is present at triple points of α grains, and the grain size and amount of the α phase are about 4–12 μm and 52%, respectively (Fig. 3b). Table 1 shows a summary of the quantitative analysis data performed for the two microstructures investigated, considering several characteristic microstructural features of the unaged and aged conditions after holding for 2, 144 and 576 h at the three different aging temperatures under investigation. These results show that the aging treatment affect the amount of α and β phases present initially in the unaged (Widmanstätten and equiaxed) microstructure; a slight increase in the amount of α phase (thus, a

Table 1. Quantitative analysis results of the microstructures of the Ti–6Al–4V

Microstructure	Parameter		Unaged	Aged								
				2 h			144 h			576 h		
				515	545	575	515	545	575	515	545	575
Widmanstätten	Colony size, μm	min	973	411	726	1061	790	899	843	1074	492	771
		max	1868	1018	1912	2339	1439	1678	1837	1277	1367	1430
	Grain boundary α thickness, μm		1–7	4–11	4–16	2–9	3–11	7–19	5–12	9–17	5–9	5–12
	Amount α phase, %		59.0	61.5	61.8	60.9	63.2	63.5	63.2	64.0	63.9	63.6
	Amount β phase, %		41.0	38.5	38.2	39.1	36.8	36.5	36.8	36.0	36.1	36.4
	α platelet thickness, μm		1–5	3–9	5–15	3–7	3–14	7–15	5–9	5–23	6–13	4–13
	Vanadium in β phase, wt %		4.2	6.0–8.0	5.7	5.6	10.0	6.9–7.7	6.2	13.0–14.0	9.0–10.6	11.6
Equiaxed	α grain size, μm		4–12	3–12	4–12	4–16	4–11	5–11	5–14	3–12	4–12	4–15
	Amount α phase, %		52.2	54.8	54.1	54.8	56.5	56.4	56.9	57.3	57.1	58.0
	Amount β phase, %		47.8	45.2	45.9	46.2	43.5	44.6	44.0	42.7	42.9	45.0
	Vanadium in β phase, wt %		9.6	12.5	14.8	12.0	18.0	14.3	18.1	18.5	22.9	20.0

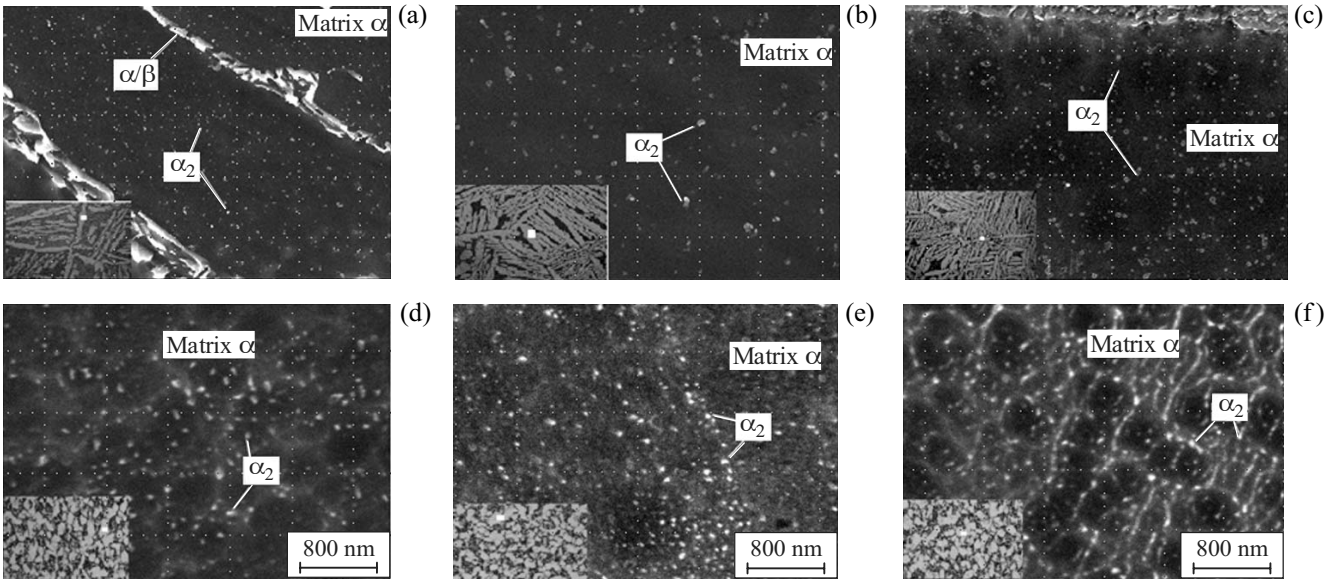

Fig. 4. SEM micrographs of the overaged Widmanstätten (a–c) and equiaxed microstructures (d–f) at 575°C for three different aging times 2, 144 and 576 h respectively, showing very fine α_2 phases homogeneously distributed in the α phase. Insets are optical micrographs (like Figs. 3a and 3b), and the regions marked by square-pointed indicate α phases, which are magnified in the SEM micrographs. Etched with Kroll's reagent.

decrease in β) is observed. In addition, there are some differences in the high-magnification SEM micrographs of the aged Widmanstätten and equiaxed microstructures as shown in Fig. 4. The insets are optical micrographs (like Fig. 4), and the regions marked by square-pointed indicate α phases, which are magnified in the SEM micrographs. Fine α_2 phases of 50–200 nm in size are homogeneously distributed in the α phase of the Widmanstätten and equiaxed microstructures.

Figure 5 displays the variation of hardness in the two initial microstructures: Widmanstätten and equiaxed as a function of different aging times at 515, 545 and 575°C. When designing these experiments it should be bore in mind that the ageing temperature should lie above the Ti_3Al solvus temperature so as to assure that the age-hardening of the α phase by Ti_3Al particles occurs. In Ti–6Al–4V alloy, the Ti_3Al solvus temperature is ~600°C, which means that aging at 500–600°C will promote the precipitation of Ti_3Al particles whereas aging at $T > 600$°C will be only a stress relieving treatment. Microhardness measurements show that the initial hardness of the Widmanstätten microstructure is higher than that of the equiaxed microstructure. Promoting these type of lamellar/lath like structures help to refine the microstructure; besides, these microstructures contain more interfaces that take part in the dislocation origination [20]. The microstructure of this type show higher hardness and, in general, better combination of mechanical properties (strength, ductility, toughness). As the ageing time increases the hardness continuously shows a rise up to 144 h and then remains roughly constant for all temperatures. Although the hardness increases with the aging time for both microstructures due to the precipitation of the α_2 particles, the hardening effect (net hardness increment) for a certain ageing time is greater for the Widmanstätten one. Finally, after 144 h of aging, the hardness seems to remain constant or even start decreasing. This effect can be related to some mechanisms which are considered in the discussion.

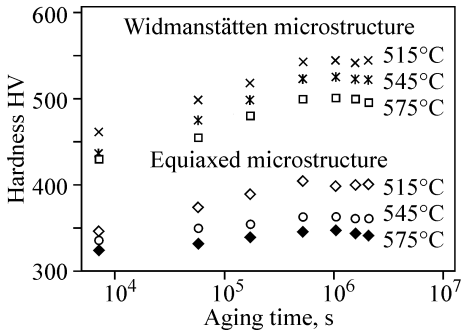

Fig. 5. Variation of hardness as a function of aging time for the three different holding temperatures (515, 545, 575°C) and the two different initial microstructures (Widmanstätten and equiaxed) under investigation.

4.2. Thermoelectric Power Measurements

Figure 6 shows the time evolution of the thermoelectric power signal for the two different microstructures and three different aging temperatures under investigation measured by both thermoelectric power methods. For all aging temperatures, there is a drop in the thermoelectric power values up to around 144 h and then the thermoelectric power increases. This is observed after using both thermoelectric power methods although, surprisingly, only the lateral gradient method is sensitive to the different initial microstructures (Widmanstätten and equiaxed). According to the lateral gradient thermoelectric method, in the case of the Widmanstätten microstructure, the thermoelectric power value for the unaged specimen is –6.53 μV/°C; while for an aging time of 144 h, the magnitude of the thermoelectric power decreases down to –7.27 μV/°C (515°C), –7.12 μV/°C (545°C) and –7.01 μV/°C (575°C). In the equiaxed microstructure, the thermoelectric power value for the unaged specimen is –6.12 μV/°C; while for an ageing time of 144 h, the magnitude of the thermoelectric power decreases down to –6.71 μV/°C (515°C), –6.60 μV/°C (545°C) and –6.47 μV/°C (575°C). On the other hand, according to the hot tip method, in the case of the Widmanstätten microstructure, the thermoelectric power value for the unaged specimen is –6.10 μV/°C; while, again, for an aging time of ~144 h, the magnitude of the thermoelectric power decreases down to –7.17 μV/°C (515°C), –6.85 μV/°C (545°C) and –6.78 μV/°C (575°C). In the equiaxed microstructure, the thermoelectric power value for the unaged specimen is –6.04 μV/°C; while for an aging time of 144 h, the magnitude of the thermoelectric power decreases down to –6.72 μV/°C (515°C), –6.58 μV/°C (545°C) and –6.53 μV/°C (575°C). Finally, the hot-tip method shows that up to 2 h (120 min) of aging time the thermoelectric power is almost independent of the microstructure, while the lateral gradient method registered a constant thermoelectric power difference of about 0.4–0.5 μV/°C between the Widmanstätten and equiaxed microstructures. These differences observed in the initial thermoelectric power values when comparing both methods are still not well understood; however, both of them are able (very sensitive) to capture the influence of ageing heat treatments on the microstructure. The fact that the main disagreement concerns with the starting values may have to do primarily with initial calibration.

Several investigations can be found in the literature concerning the influence of ageing on thermoelectric power in Fe-, Al-, Cu- and Zr-based alloys [9, 21–34]. During this process, the thermoelectric power is governed by the specific thermoelectric power value of every solute atom present in solid solution and by the intrinsic effect of precipitates formed. According to the literature, the effect of solutes can be positive or negative. In Zr-based alloys, precipitation reactions seem to increase the thermoelectric power (removal of Fe, Cr and Ni from solid solution) [21]. Similarly, in steels, the thermoelectric power has been observed to decrease due to the solid solution of atoms like C, N, Cu, Cr, Ti [9, 22–31]; however contrary to these investigations, it was observed that the effect of Mo on iron is positive [29], result that has been supported by a recent paper on the ageing behavior of a maraging steel C250, in which Mo seems to have a positive influence as-well [30]. In Al- and Cu-based alloys, the thermoelectric power shows a more complex behavior; it decreases [32–35] or increases [32–34] depending on the precipitated species. In this latter type alloys, the intrinsic effect seems to have an important effect.

In spite of all these studies, no work could be found in the literature concerning the influence of solutes in

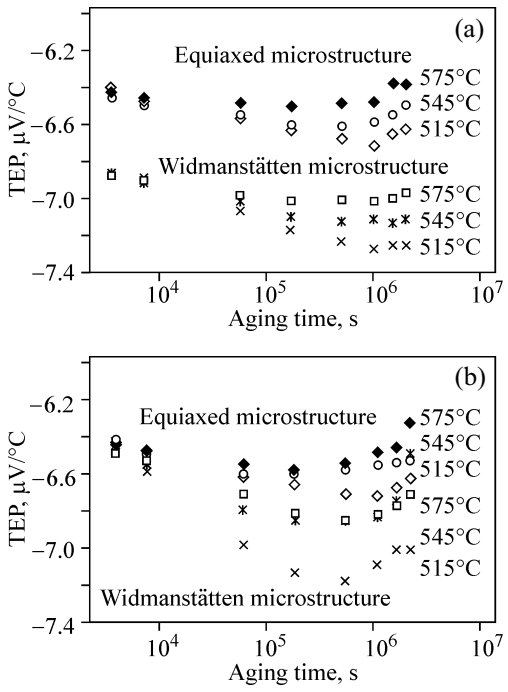

Fig. 6. Thermoelectric power measurements using the lateral gradient thermoelectric method (a) and the hot tip thermoelectric method (b) in the Widmanstätten and equiaxed microstructures overaged at 515, 545 and 575°C for different aging times.

solid solution and/or precipitation on the thermoelectric power in Ti-based alloys. As it has been shown in this work, during ageing the formation of coherent nanometer-sized α_2 (Ti_3Al) particles takes place (Fig. 4); this is associated with a thermoelectric power decrease up to ~144 h and, then, a gradual increase for longer times. The results depicted in Table I highlight that besides precipitation, other changes take place in the microstructures are: (i) there is an increase in the amount of α phase (4–5%) up to 144 h which then remains roughly constant; (ii) the amount of vanadium in the β phase increases continuously in the Widmanstätten microstructure from 4.20 wt % in the unaged sample, up to 9–14 wt % in the samples aged for 576 h (Table 1); while in the equiaxed microstructure it increases from 9.6 wt % in the unaged condition up to values of 18.5–22.9 wt % in the samples aged for 576 h; (iii) besides, in the Widmanstätten-like microstructure the α platelet size increases significantly and continuously during ageing, from 1–5 μm in the unaged samples up to 5–23 μm in some aged ones; in the equiaxed microstructure there is also an increase in the average size of the α phase. Finally, the main difference between the Widmanstätten and the equiaxed initial microstructures (apart from the morphology of the α phase) is the amount of α phase (lower for the equiaxed): according to the lateral gradient method, the thermoelectric power of the initial microstructure decreases around 0.4–0.5 μV/°C due to an increase in the amount of α phase of around 6.8% (although the hot tip method does not differentiate this two microstructures). Thus, based on this later result (higher amount of α phase, lower thermoelectric power) one could suggest that the initial decrease in the thermoelectric power up to 144 h could be due to the increase in the amount of the α phase (4–5%) during ageing. However, other factors should be also considered: (i) the intrinsic effect of the nanometer size precipitates would introduce internal stresses in the matrix which act as additional scattering sites for electrons (decrease in thermoelectric power) [18]; (ii) the enrichment in vanadium of the β phase will have an effect; (iii) in addition, in the Widmanstätten microstructure, the platelet size increases in size significantly with the ageing time and, thus, the number density of grain/phase boundaries decreases (that serve as scattering points for electron diffusion), which should have a positive (increase) effect on the thermoelectric power. In the second stage of the aging process, above ~144 h, the growth of the α phase due to ageing seems to reach equilibrium, but the precipitation of the α_2 nanophase becomes very pronounced in the α phase (Fig. 4). The formation of the α_2 phase depletes the matrix in solutes like Al and Ti, which seems to have a strong positive effect on the thermoelectric power (increase) beyond 144 h. Besides, as precipitates grow in size with the ageing time, they will probably become incoherent and the intrinsic negative effect likely present for shorter aging times will probably disappear, resulting in a further increase in thermoelectric power. Further studies on the influence of the aging process in Ti–6Al–4V on the thermoelectric power measurements should be considered in the future to support this investigation.

5. DISCUSSION

The present research is mainly aimed at achieving the optimum precipitation of nanometer-sized α_2 (Ti_3Al) particles in an overaged Ti–6Al–4V alloy with the Widmanstätten and equiaxed microstructure. Precipitation of α_2 (Ti_3Al) particles was monitored using thermoelectric power measurements. It was necessary to classify all regularities of TEM and Ti_3Al particle relations to have an optimum effect of the precipitation process.

As Ti_3Al particles precipitate within the α phase, it is very important to understand the conditions and role of the Widmanstätten, equiaxed and α phase structures in the Ti–6Al–4V alloy.

The Widmanstätten structure is most preferential in the Ti–6Al–4V alloy. It gives a reinforcing effect in misoriented grains of the polycrystal, which ensures high hardness of the alloy. The developed system of interfaces provides a high generation of dislocations and high plasticity of the alloy [20]. The possibility of reversible transformation of the ω phase and α/β phase under dynamic loading [36, 37] explains high fracture toughness of this microstructure. A high volume fraction of the α-phase in the Widmanstätten microstructure, in which the α_2 (Ti_3Al) precipitation is possible, causes the alloy hardness to sufficiently increase during its overaging (Fig. 5).

All the mentioned effects are less pronounced or lack in the equiaxed microstructure (for example, the reinforcing effect). However, the very high interaction of internal stress fields related to equiaxed particles governs the development of dynamic rotations in the particle distribution at the aging time 576 h (Fig. 4f). This is a rotational mechanism of relaxation, which appears as an individual stage in the dependences of

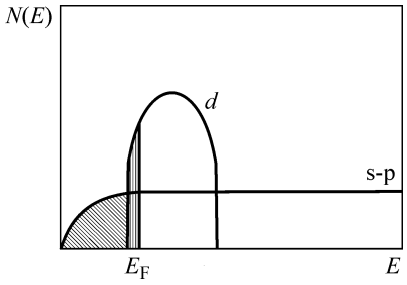

Fig. 7. Schematic curves of the density of states $N(E)$ as a function of energy E for titanium.

hardness and thermoelectric power on the aging time. The additional plausible explanation could be a changed mechanism of precipitation hardening because, when growing in size, they become incoherent and the interaction between dislocations and precipitates changes from shearing to Orowan one [38].

In full accordance with the mechanical behavior and structural transformations, an increase in aging time changes thermoelectric power (Fig. 6). Negative thermoelectric power is related to the electronic density of states at the Fermi level, which is illustrated in Fig. 7 for Ti. The (s-p) and (3d) bands are overlapped in Ti and have the common Fermi energy and $N(E_F)$. It allows a redistribution of (s-p)- and d-electrons in the electron spectrum of Ti and its alloys.

A clear separation of α/β and α phases in the Widmanstätten microstructure and the presence of three d-electrons in vanadium (Ti has only two d-electrons) govern more negative thermoelectric power values in the Widmanstätten microstructure as compared to those in the equiaxed one. With increasing aging time, the precipitation of Ti_3Al is accompanied by an increase in the electronic density of states $N(E_F)$ at the Fermi level. This increases electronegative values of thermoelectric power in both the microstructures. The final stage of the thermoelectric power increase in the thermoelectric power aging time curves can be related to the appearance of dynamic rotations in the distribution of Ti_3Al particles and loss of their coherency with the α phase, which decreases the general contribution of Ti_3Al precipitation to thermoelectric power and mechanical characteristics of the alloy.

The thermoelectric power value is a very sensitive characteristic of structural states in the titanium alloy. However, the correct analysis of the observed mechanisms requires the knowledge of corresponding changes in the electron subsystem of the heterogeneous material.

6. CONCLUSIONS

This work investigates the relationship between the thermoelectric power and microstructural changes in the Widmanstätten and equiaxed microstructures during aging of a Ti–6Al–4V alloy using two thermoelectric methods: lateral gradient and hot tip. The lateral thermoelectric method exhibited a stronger interaction with the initial microstructural features as compared to that of the hot tip thermoelectric method. In particular, this phenomenon was observed for the significant separation between the thermoelectric thermoelectric power data obtained. However, the present study reveals an unusual sensitivity of the thermoelectric power value to the aging state of Ti–6Al–4V alloy. Following 144 h of aging at the three heat treatment temperatures (515, 545, 575°C) the thermoelectric power value of the titanium alloy showed a change of –0.9 μV/°C which is significantly different to other aged alloys. In this Ti alloy, this decrease is probably due to the increase in the volume fraction of the α phase and the intrinsic effect of the α_2 nanoprecipitates. Besides, other effects like the increase in the platelet size and the β phase enrichment in vanadium could be also contributing to the thermoelectric power value during the initial stages of ageing. Finally, the increase in thermoelectric power for long times is attributed to the precipitation of nanometer-sized α_2 (Ti_3Al) particles inside α phases and to the loss of coherency of the α_2 precipitates for long ageing times. On the other hand, the microhardness measurements show the strong strengthening effect of this precipitates up to 144 h. However, for longer aging times, the development of dynamic rotations in α_2 (Ti_3Al) distribution and the increase in size of these precipitates leads to a plateau in the hardness, probably due to a loss of coherency of the precipitates.

ACKNOWLEDGMENTS

This work was performed at UMSNH-MEXICO and CENIM-CSIC-ESPANA with funding from CONACYT-MEXICO under project CB-80883. The author H. Carreon wishes to thank CONACYT (Mexico) for the financial support during the sabbatical in CENIM-CSIC D. San Martin would like to acknowledge the financial support from the Ministerio de Economia y Competitividad (Project No. MAT 2010-19522). The authors are grateful to Mr. J. Vara (CENIM) for the experimental support with the heat treatments and part of the thermoelectric power measurements.

REFERENCES

1. Mier, M. and Mukherjee, A.K., Effects of Microstructural Morphology on Quasi-Static and Dynamic Deformation Behavior of Ti–6Al–4V Alloy, *Scr. Metall. Mater*., 1990, vol. 24, no. 2, pp. 331–336.
2. Yadav, S. and Ramesh, K.T., The Mechanical Properties of Tungsten-Based Composites at Very High Strain Rates, *Mater. Sci. Eng. A*, 1995, vol. 203, pp. 140–153.
3. Lee, D.G., Lee, Y.H., Lee, C.S., and Lee, S., Effects of Volume Fraction of Tempered Martensite on Dynamic Deformation Properties of a Ti-6Al-4V Alloy Having a Bimodal Microstructure, *Metall. Mater. Trans. A*, 2005, vol. 36, pp. 741–748.
4. Neelakantan, S., San Martin, D., Rivera-Díaz-Del-Castillo, P.E.J., and van der Zwaag, S., Plasticity Induced Transformation in a Metastable β Ti-1023 Alloy by Controlled Heat Treatments, *Mater. Sci. Technol*., 2009, vol. 25, no. 11, pp. 1351–1358.
5. Gysler, A. and Lutjering, G., Influence of Test Temperature and Microstructure on the Tensile Properties of Titanium Alloys, *Metall. Trans. A*, 1982, vol. 13, pp. 1435–1443.
6. Lee, D.G., Lee, S., Lee, C.S., and Hur, S., Effects of Microstructural Factors on Quasi-Static and Dynamic Deformation Behaviors of Ti-6Al-4V Alloys with Widmanstätten Structures, *Metall. Mater. Trans. A*, 2003, vol. 34, pp. 2541–2548.
7. Lee, D.G., Lee, S., and Lee, C.S., Quasi-Static and Dynamic Deformation Behavior of Ti–6Al–4V Alloy Containing Fine α_2-Ti_3Al Precipitates, *Mater. Sci. Eng. A*, 2004, vol. 366, pp. 25–37.
8. Mitra, R., *Structural Intermetallics and Intermetallic Matrix Composites*, Boca Raton: CRC Press, Taylor & Francis Group, 2015, pp. 16–18.
9. Caballero, F.G., Capdevila, C., Alvarez, L.F., and Garcia de Andres, C., Thermoelectric Power Studies on a Martensitic Stainless Steel, *Scripta Mater*., 2004, vol. 50, no. 7, pp. 1061–1066.
10. Ferrer, J.P., de Cock, T., Capdevila, C., Caballero, F.G., and Garcia de Andres, C., Comparison of the Annealing Behaviour between Cold and Warm Rolled ELC Steels by Thermoelectric Power Measurements, *Acta Mater*., 2007, vol. 55, no. 6, pp. 2075–2083.
11. Pollock, D.D., *Thermoelectricity*, Philadelphia, PA: ASTM, 1985, pp. 39–41.
12. Carreon, H., Barriuso, S., Lieblich, M., Gonzalez, J.L., Jimenez, J.A., and Caballero, F.G., Significance of the Contacting and No Contacting Thermoelectric Power Measurements Applied to Grit Blasted Medical Ti6Al4V, *Mater. Sci. Eng. C*, 2013, vol. 33, pp. 1417–1422.
13. Carreon, H., Barriuso, S., Barrera, G., Gonzalez, J.L., and Caballero, F.G., Assessment of Blasting Induced Effects on Medical 316 LVM Stainless Steel by Contacting and Non-Contacting Thermoelectric Power Techniques, *Surf. Coat. Tech*., 2012, vol. 206, pp. 2941–2946.
14. Kawaguchi, Y. and Yamanaka, S., Applications of Thermoelectric Power Measurement to Deterioration Diagnosis of Nuclear Material and Its Principle, *J. Nondestr. Eval*., 2004, vol. 23, no. 2, pp. 65–76.
15. Hu, J. and Nagy, P.B., On the Role of Interfase Imperfections in Thermoelectric Nondestructive Material Characterization, *Appl. Phys. Lett*., 1998, vol. 73, no. 4, pp. 467–469.
16. Maslov, K. and Kinra, V.K., Noncontact Thermoelectric NDT for Alloy Microstructural Analysis, *Mater. Eval*., 2001, vol. 59, pp. 1081–1084.
17. Welsch, G., Lutjering, G., Gazioglu, K., and Bunk, W., Deformation Characteristics of Age Hardened Ti-6Al-4V, *Metall. Trans. A*, 1997, vol. 18, pp. 169–177.
18. Celada Casero, C. and San Martin, D., Austenite Formation in a Cold-Rolled Semi-Austenitic Stainless Steel, *Metall. Mater. Trans. A*, 2014, vol. 45, no. 4, pp. 1767–1777.
19. Lutjering, G., Influence of Processing on Microstructure and Mechanical Properties of $(\alpha+\beta)$ Titanium Alloys, *Mater. Sci. Eng. A*, 1998, vol. 243, no. 2, pp. 32–45.
20. Panin, V.E. and Egorushkin, V.E., Basic Physical Mesomechanics of Plastic Deformation and Fracture of Solids as Hierarchically Organized Nonlinear Systems, *Phys. Mesomech*., 2015, vol. 18, no. 4, pp. 377–390.
21. Loucif, K., Borrelly, R., and Merle, P., On the Thermoelectric Power Variation According to Temperature of Zirconium Alloys and Its Possible Application to the Estimation of the Amount of Solubility Variations of Iron and Chromium in Zircalloy, *J. Nucl. Mater*., 1993, vol. 202, no. 1, pp. 193–196.
22. Benkirat, D., Merle, P., and Borrelly, R., Effects of Precipitation on the Thermoelectric Power of Iron-Carbon Alloys, *Acta Metall*., 1988, vol. 36, no. 3, pp. 613–620.
23. Brahmi, A. and Borrelly, R., Study of Aluminium Nitride Precipitation in Pure FeAlN Alloy by Thermoelectric Power Measurements, *Acta Mater*., 1997, vol. 45, no. 5, pp. 1889–1897.
24. Perez, M., Sidoroff, C., Vincent, A., and Esnouf, C., Microstructural Evolution of Martensitic $100Cr_6$ Bearing Steel during Tempering: From Thermoelectric Power Measurements to the Prediction of Dimensional Changes, *Acta Mater*., 2009, vol. 57, no. 11, pp. 3170–3181.
25. Massardier, V., Lavaire, N., Soler, M., and Merlin, J., Comparison of the Evaluation of the Carbon Content in Solid Solution in Extra-Mild Steels by Thermoelectric Power and by Internal Friction, *Scripta Mater*., 2004, vol. 50, no. 12, pp. 1435–1439.
26. Rana, R., Singh, S.B., and Mohanty, O.N., Thermoelectric Power Studies of Copper Precipitation in a New Interstitial-Free Steel, *Scripta Mater*., 2006, vol. 55, no. 12, pp. 1107–1110.
27. Caballero, F.G., Garcia-Junceda, A., Capdevila, C., and Garcia de Andres, C., Precipitation of $M_{23}C_6$ Carbides: Thermoelectric Power Measurements, *Scripta Mater*., 2005, vol. 52, no. 6, pp. 501–505.

28. Tkalcec, I., Azcoitia, C., Crevoiserat, S., and Mari, D., Tempering Effects on a Martensitic High Carbon Steel, *Mater. Sci. Eng. A*., 2004, vol. 387, pp. 352–356.
29. Houze, M., Kleber, X., Fouquet, F., and Delnondedieu, M., Study of Molybdenum Precipitation in Steels Using Thermoelectric Power Measurement, *Scripta Mater*., 2004, vol. 51, no. 12, pp. 1171–1176.
30. Pinkas, M., Moshka, O., Okavi, S., Shmuelevitsh, M., Gelbstein, Y., Froumin, N., and Meshi, L., The Origin of the Effect of Aging on the Thermoelectric Power of Maraging C250 Steel, *J. Mater. Sci*., 2015, vol. 50, pp. 7698–7704.
31. Celada Casero, C., *Solid-Solid Phase Transformations in a Metastable Stainless Steel: Microstructural Control and Mechanical Properties: PhD Thesis*, Madrid: Complutense University of Madrid, 2015.
32. Pelletier, J.M., Vigier, G., Mal, C., and Borrelly, R., Influence of the Initial Stages of Precipitation on the Electrical Properties of Cu–Be Alloys, *Acta Metall*., 1983, vol. 31, pp. 1491–1498.
33. Pelletier, J.M., Virgier, G., Merlin, J., Merle, P., Fouquet, F., and Borrelly, R., Precipitation Effects on Thermopower in Al–Cu Alloys, *Acta Metall*., 1984, vol. 32, no. 7, pp. 1069–1078.
34. Gaffar, M.A., Gaber, A., Mostafa, M.S., and Abo Zeid, E.F., The Effect of Cu Addition on the Thermoelectric Power and Electrical Resistivity of Al–Mg–Si Balanced Alloy: A Correlation Study, *Mater. Sci. Eng. A*, 2007, vol. 465, no. 1, pp. 274–282.
35. Gutierrez-Urrutia, I., Study of Isothermal δ′(Al_3Li) Precipitation in an Al–Li Alloy by Thermoelectric Power, *J. Mater. Sci*., 2011, vol. 46, pp. 3144–3150.
36. Panin, V.E., Egorushkin, V.E., Panin, A.V., and Chernyavskii, A.G., Plastic Distortion as a Fundamental Mechanism in Nonlinear Mesomechanics of Plastic Deformation and Fracture, *Phys. Mesomech*., 2016, vol. 19, no. 3, pp. 255–268.
37. Panin, V.E., Panin, A.V., Pochivalov, Yu.I., Elsukova, T.F., and Shugurov, A.R., Scale Invariance of Structural Transformations in Plastically Deformed Nanostructured Solids, *Phys. Mesomech*., 2017, vol. 20, no. 1, pp. 55–68.
38. Martin, J.W., *Precipitation Hardening: Theory and Applications*, Oxford: Pergamon Press, 2012.